Analysis of On- and Off-Line Optimized Predictive Current Controllers for PWM Converter Systems

Johann W. Kolar, *Member, IEEE*, Hans Ertl, and Franz C. Zach, *Member, IEEE*

***Abstract*—This paper treats the problem of ON-OFF current control for coupling of a dc voltage system with a three-phase (polyphase) ac voltage system via a pulsewidth modulated (PWM) converter. There the ac voltage represents (according to the directions of the energy flow which is possible in both directions) either the counter emf of an ac machine or the three-phase power supply system (mains). The following control concepts are investigated by digital computer simulation:**

1) a simple hysteresis controller:

2) a predictive controller with ON-line optimization (optimization with respect to minimum switching frequency) and

3) a controller based on OFF-line optimization (using a switching table). It is shown that for the system analyzed here, the relatively involved (concerning its realization) predictive controller can be replaced by a switching table of very limited size. For rating of the treated controllers the switching frequency (at the same rms value of the current control error) as a function of the rms voltage of the ac system and the other system parameters is used.

I. INTRODUCTION

ONE of the main areas of interest in power electronics as applied to modern drive systems is the supply of ac machines from a dc voltage link via a PWM inverter. The reversed energy flow (i.e., from the ac side to the dc side) leads to a structure called forced commutated rectifier, FCR [1]. Also the drive system mentioned earlier only represents an application of a general power electronic system for coupling of two voltage systems (dc and ac) which (as shown in Fig. 1) for the following can be imagined by ideal ac or dc voltage sources.

The main state variables of the described power electronic system with respect to physics and technology are given by the currents of the ac side. This is because they determine the energy flow in the system (considering their phase relationship with respect to the voltage) and the maximum current stress of the switching device. It is therefore obvious that the control concept for the system should incorporate these characteristic variables. In this paper the problem of current control of the mentioned power electronic system is treated exclusively.

In order to limit the extent of this paper only ON-OFF control characteristics are considered. For these the switching instants are asynchronous (i.e., they are not correlated to the period of the ac voltage); this can be explained by the fact that the current is only controlled (guided) within a deadband around its reference value. This results in not exactly defined fundamentals (with regard to amplitude, frequency and phase) of the converter output ac voltage and current. An alternative to this (asynchronous) control concept as treated here is given by application of a pulse pattern generator for which the modulation depth and the phase of the converter output voltage are controlled dependent on the current control error. Then there are possible synchronous as well as asynchronous modi of operation. The former is characterized by a discrete frequency spectrum.

The classical (and simplest) realization of an ON-OFF controller for a three phase system is given by three independent hysteresis phase current controllers. The voltage between the virtual center point of the dc link voltage U_Z (I in Fig. 1) and the star (neutral) point of the ac system (II in Fig. 1) is given by the switching status k_I ($k_I = 0..7$). The voltage between I and II is $u_0 = (u_{U.R} + u_{U.S} + u_{U.T})/3$ where $u_{U.R}$, $u_{U.S}$, $u_{U.T}$ are the phase voltages of the converter with respect to point I. Therefore the change of the switching status of one phase effects the other phases. Because this coupling effect is not *a priori* considered by the simplest ON-OFF control system as described before, among other properties a maximum current control error of twice the deadband width results. If the switching actions of the different phases are coordinated the current can be kept within the dead-band. Furthermore then also an optimization (as described, e.g., in [2]) is possible aiming at a minimum switching frequency; another optimization criterion is, e.g., minimization of the rms value of the current control error. Because such an optimization basically is only meaningful for stationary operating conditions a second control system has to be superimposed on this optimized controller to handle transient conditions (see Sections IV and V).

In this paper the stationary operating conditions of a simple ON-OFF controller, of a controller based on OFF-line optimization (using a switching table) and of an ON-line optimizing (predictive) ON-OFF current controller are investigated and compared by digital computer simulation.

Manuscript received June 23, 1987.

The authors are with the Technical University of Vienna, Power Electronics Section, Gusshausstrasse 27-29, A—1040, Vienna, Austria.

IEEE Log Number 9100519.

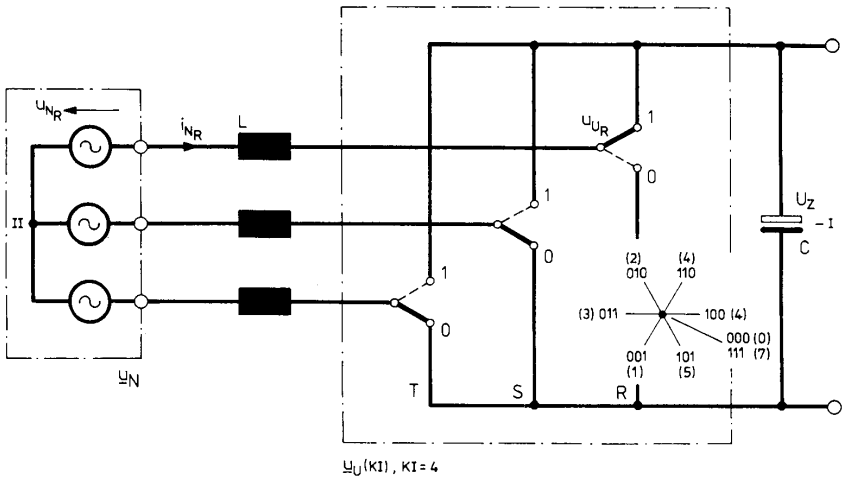

Fig. 1. Basic structure of interconnection of an ac and a dc system via a pulsewidth modulated (PWM) converter. One converter leg (e.g., 2 power transistors with antiparallel freewheeling diodes) can be symbolized by simple two-pole switch connecting either positive or the negative dc link bar to the respective ac phase.

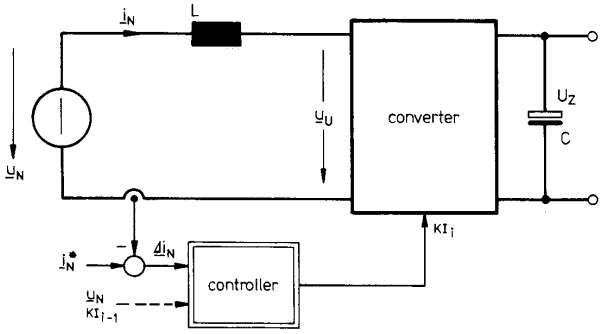

Fig. 2. Control structure of system (Fig. 1) based on space vector description of the state variables.

II. Description of the System by Space Vectors

According to Fig. 2 the space vector differential equation is given by

$$\underline{u}_N = \underline{u}_U(k_I) + L\frac{d\underline{i}_N}{dt} \tag{1}$$

where $\underline{i}_N$ is the ac current (called also mains current in the following), $\underline{u}_N$ is the mains voltage and $\underline{u}_U(k_I)$ is the converter output (ac side) voltage (switching status k_I; denoted by KI or K in the figures). We define

$$\Delta\underline{i}_N = \underline{i}_N^* - \underline{i}_N \tag{2}$$

as the current control error. This yields with (1):

$$L\frac{d\Delta\underline{i}_N}{dt} = \underline{u}_U(k_I) - \left(\underline{u}_N - L\frac{d\underline{i}_N^*}{dt}\right)$$

$$= \underline{u}_U(k_I) - \underline{u}_{U,i}. \tag{3}$$

In (3), $\underline{u}_{U,i}$ represents that (ideal) converter output voltage which on one hand forms the counter voltage to the mains and on the other hand would effect a current change in L according to the reference value change. There are only six different nonzero converter output voltage vectors of equal magnitude (with a direction depending on the switching status k_I)

$$|\underline{u}_U(k_I)| = \tfrac{2}{3}U_Z \qquad k_I = 1 \cdots 6. \tag{4}$$

Together with both zero vectors $k_I = 0$ and $k_I = 7$, there exist altogether seven vectors $d\Delta\underline{i}_N(k_I)/dt$ being different with respect to absolute value and direction (Fig. 3). An influence on the rate of change of the current control error $(d\Delta\underline{i}_N/dt)$ is given here by the parameters k_I, U_z, $\underline{u}_N$, L, $\underline{i}_N$ and ω_N. As can be easily estimated, for practical applications the inductive voltage drop $L\,a\underline{i}_N/dt$ can be neglected in comparison to $\underline{u}_N$ in many cases (see Fig. 3: $\Delta\phi \to 0$).

Under stationary operating conditions one can assume sinusoidal quantities forming $\underline{u}_N$ and $\underline{i}_N^*$. There the space vector of the current control error $\Delta\,\underline{i}_N$ due to (2) is rep-

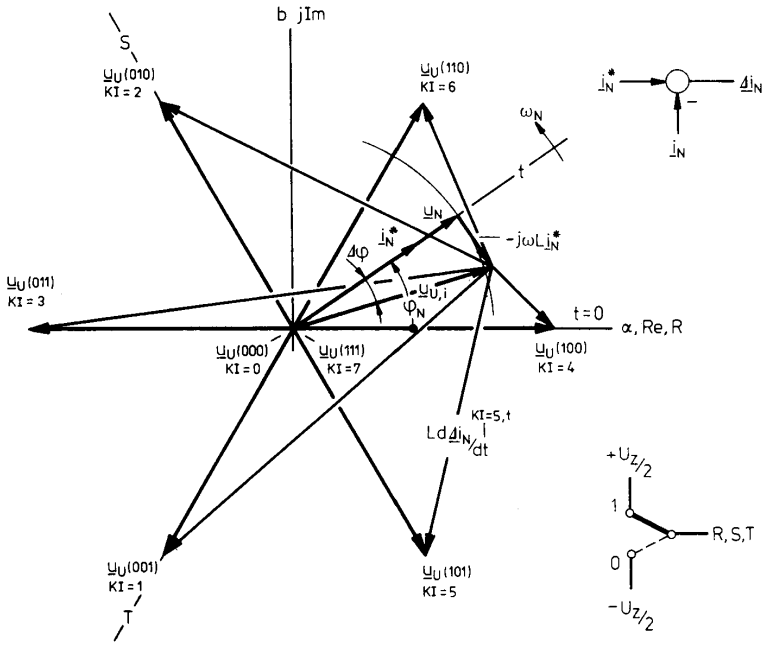

Fig. 3. System state vectors.

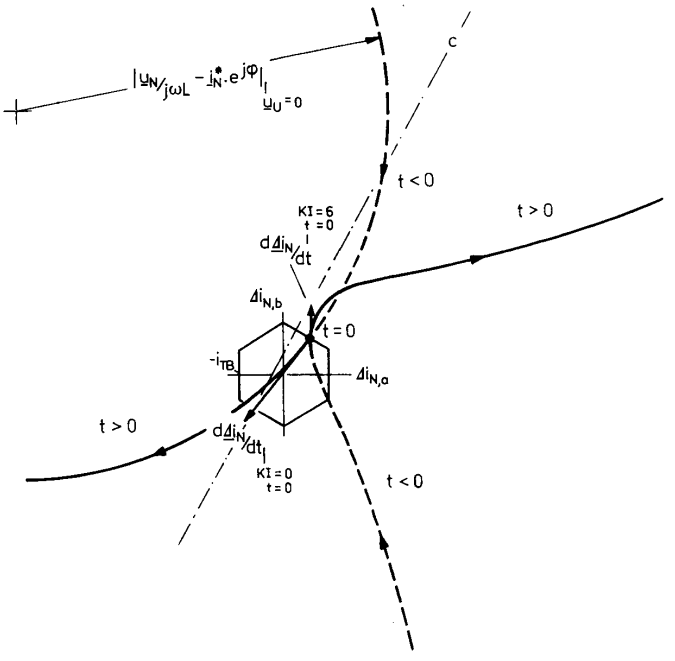

Fig. 4. Trajectories of the current control error $\Delta\underline{i}_N$ shown for $|\underline{u}_U|$ close to $|\underline{u}_N|$. The "axis" C is parallel to $\underline{u}_U(k_I)$ for k_I = 0, 7. For i_{TB} and hexagon see section 3.

resented in a coordinate system whose origin lies in the tip of $\underline{i}_N^*$. The trajectories of $\Delta\underline{i}_N(k_I)$ are trochoids which degenerate to circles for $k_I = 0$ or $k_I = 7$ (Fig. 4).

The rms value of Δi_N eff of the current ripple which is used to compare the different current controllers can be calculated from the space vector $\Delta\underline{i}_N$. At first we define:

$$\sum\Delta i^2 = \Delta i_{N,R}^2 + \Delta i_{N,S}^2 + \Delta i_{N,T}^2. \tag{5}$$

Equation (5) characterizes the power dissipation of the system due to current control errors and can also be expressed by the space vector $\Delta \underline{i}_N$:

$$\sum \Delta i^2 = \tfrac{3}{2} |\Delta \underline{i}_N|^2. \tag{6}$$

Accordingly,

$$\Delta i_{N_{\text{eff}}} = \sqrt{\frac{1}{T} \int_0^T \frac{1}{2} |\Delta \underline{i}_N|^2 \, dt} \tag{7}$$

is used as a quality criterion. For converter switching frequencies in the kilohertz range for rms value calculations the trajectories of $\Delta \underline{i}_N$ can be replaced by straight lines with very good approximation (the error lies in the 0.1 percent range).

Because, as mentioned before, for the simple hysteresis controller the maximum control error is larger than the deadband (exactly twice the deadband) a (time-) statistics is established considering the magnitude of the current control error for judging the frequency (probability) of leaving the deadband. There the sum of such time intervals where $|\Delta \underline{i}_N|$ lies within the interval $[I, I + \Delta I]$ is related to the entire time and divided by the interval width ΔI. This quotient $p(I)$ represents (in a statistical sense) the distribution density of the magnitude of $\Delta \underline{i}_N$. From this function one can also draw conclusions with respect to the occurring rms value $\Delta \underline{i}_{N,\text{eff}}$ because $p(I)$ weighs the square of the magnitude of the space vector $\Delta \underline{i}_N$. The probability of the occurrence of a magnitude $I < I'$ thereby follows as

$$W(I') = \int_0^{I'} p(I) \, dI \tag{8}$$

Remark: Here, the current control errors are assumed as stochastic signals in the sense of signal theory. Therefore one can only give a continuous power density spectrum for them which could be obtained by a Fourier transform of the auto correlation function. However, in this paper the analysis in the frequency domain is not persued further.

Besides the mathematical advantages of the space vector representation a very clear description of the system behavior is made possible. E.g., the deadbands around the phase current reference values are transformed into stripes lying perpendicular to the respective phase axis (see Fig. 5, there shown for phase R). The common area of these stripes (i.e., the control errors of all three phases are smaller than the deadband width) results in a hexagon being characteristic for three-phase ON-OFF controllers (see Figs. 7, 17). The tip of the reference value space vector lies in the center of the hexagon. Basically one could define arbitrary areas instead of the hexagon if the control concept is based on a space vector representation of the control error (e.g., such as in [2]). Contrary to such areas only the hexagon guarantees the full use of the allowable phase current control error. The corners of the hexagon represent the simultaneous reaching of the deadband limits (one upper and one lower limit) in two phases.

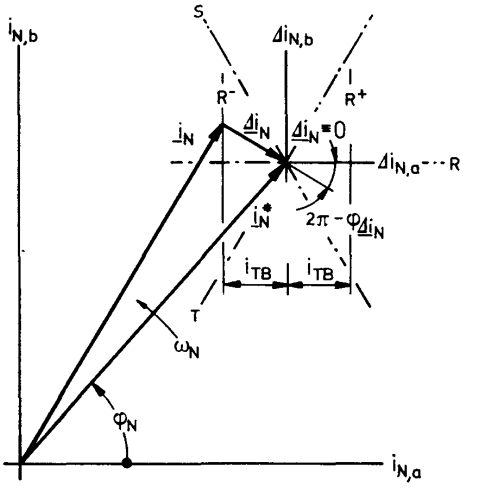

Fig. 5. Current space vectors and control error stripe for phase *R*.

If one defines, e.g., the "inner circle" of the hexagon (the circle touching all six sides of the hexagon) as control error area, there results the same maximum value of the phase currents; however the smaller area leads to a higher switching frequency of the system.

III. Hysteresis Current Controller

For this simplest form of ON-OFF current control the converter switching status is given by three independent phase current controllers (Fig. 6). Therefore, a maximum control error results being twice the deadband width. This is because the switching action of the phase where the deadband is left can only result in reentering the deadband if the switching status of the other two phases does make this possible. (This is obviously caused by the three phase structure of the system.)

An unbiased comparison of the hysteresis controller with other ON-OFF controllers therefore has to consider the maximum control error reached; the comparison cannot be simply based on equal deadband widths because the implicitly tolerated larger control error results in a lower switching frequency than for exact observance of the deadband. It is meaningful, however, to compare the switching frequencies, e.g., for equal rms value of the control error. A detailed analysis of the simple ON-OFF current controller is given in [3].

IV. Predictive Controller

As described in Section III the control error can assume a maximum value of twice the deadband width in the case of simple hysteresis control. This is due to the independent phase current controllers. If $\Delta \underline{i}_N$ has to be controlled such that it remains within the i_{TB}-tolerance region (hexagon), the reaction of the whole system to a switching decision has to be considered before it is "executed" by the converter. Certainly excluded should be that (old)

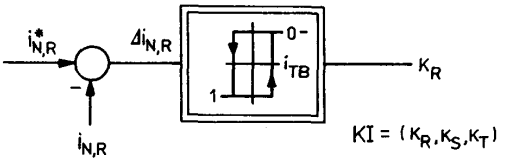

Fig. 6. Hysteresis current controller (shown for phase R).

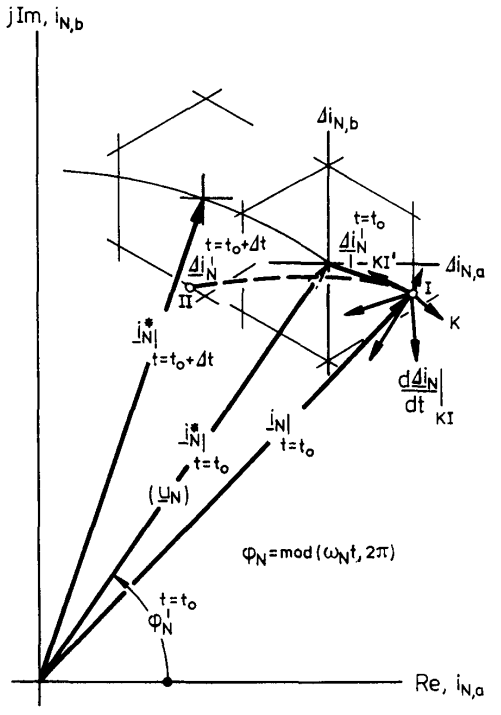

Fig. 7. Operation of predictive controller: For $t = t_0$ $\Delta \underline{i}_N$ reaches the tolerance area limit in I. The changing of the converter switching status from k to k_I leads $\Delta \underline{i}_N$ back into the hexagon; then $\Delta \underline{i}_N$ does not leave it until $\Delta t = t(k_I)$ in II.

switching state k which actually makes necessary a converter switching status change (because the relevant trajectory leaves the hexagon). In general more than one of the remaining seven (only six for $k = 0$ or $k = 7$) possible switching states will lead the control error back into the hexagon (Fig. 7). Among these a selection has to be made in an optimal sense.

One possible optimization criterion is, e.g., the maximization of the dwell time $[t(k_I)]$ of the trajectory within the hexagon, weighted by the number of necessary switchings $n(k, k_I)$ to get from the old converter switching status k to the new one k_I (Fig. 8). This acts as a switching frequency minimization. But via $n(k, k_I)/t(k_I)$ only the local switching frequency is minimized (as, e.g., in a steepest descent method) and does not necessarily mean that the global minimum will be found (compare I in Fig. 8). On the other hand, a global optimization in

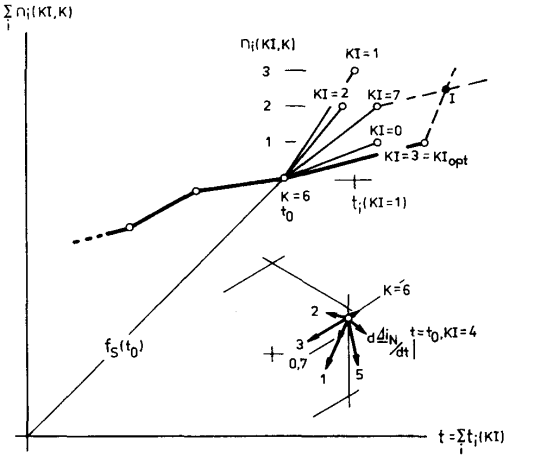

Fig. 8. Predictive controller: Minimization of f_s; $t(k_I)$ weighted by $n(k, k_I)$ corresponds to reciprocal value of "local" switching frequency in $t = t_0$. The "global" switching frequency $f_s(t_0)$ is determined by $\Sigma[n(k, k_I)], \Sigma t_i(ki)$.

practice cannot be performed due to the enormous computational effort connected herewith.

Another optimization criterion could be, e.g., to minimize the (local) contribution of the considered part of the trajectory to the rms value of the control error. Also in this case the optimization criterion can be mathematically formulated easily.

The control of $\Delta \underline{i}_N$ within the tolerance area (which is the side condition of the optimization) can only be guaranteed if at least one of the $[d(\Delta \underline{i}_N)/dt]k_I$ leads back into the hexagon. From this the controllability margin (being in general dependent on the geometrical form of the tolerance area) of the predictive controller can be derived (Fig. 9). The optimization, of course, is only possible if at least two k_I exist fulfilling the constraint. As the analysis of the switching decisions chosen by the optimization procedure shows, for $|\underline{u}_N|$ close to $|\underline{u}_U|$ — relatively independent of the weighting by $n(k, k_I)$ — frequently such switching states are selected where the converter output voltage vector is close to the mains voltage; this results in a correspondingly low magnitude of the $d(\Delta \underline{i}_N)/dt$. In the case of $|\underline{u}_N| \ll |\underline{u}_U|$ the $[d(\Delta \underline{i}_N)/dt]k_I$ show about equal magnitudes (with exception of the freewheeling state which is taken on in a preferred manner). The selection of the switching decision (besides $k_I = 0.7$) then is essentially influenced by the $n(k, k_I)$.

The investigation in this section is limited to the stationary operating behavior of the predictive controller. In a dynamic sense its function is limited by the converter voltage margin. This is because with (3) for high $d(\underline{i}^*_N)/dt$ the value of $d(\Delta \underline{i}_N)/dt$ is mainly determined by the reference value. To handle this operating condition a further control concept (e.g., a hysteresis controller) is to be superimposed onto the predictive controller; this controller brings the transient (possibly large) control error back into the tolerance region.

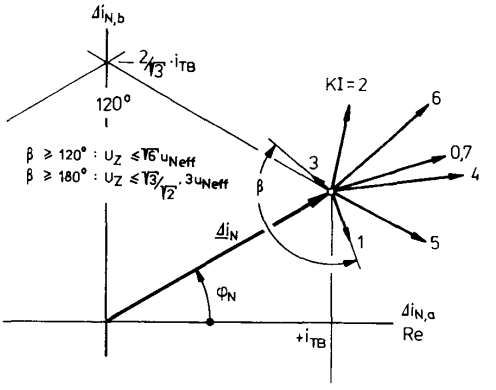

Fig. 9. Predictive controller controllability margin: for $\beta > 120°$ possibly (dependent on $\underline{u}_N$) no trajectory guides $\Delta\underline{i}_N$ back into hexagon from one of its corners. If $\Delta\underline{i}_N$ lies on edges of hexagon $\beta < 180°$ is sufficient that there is at least one trajectory leading back into hexagon.

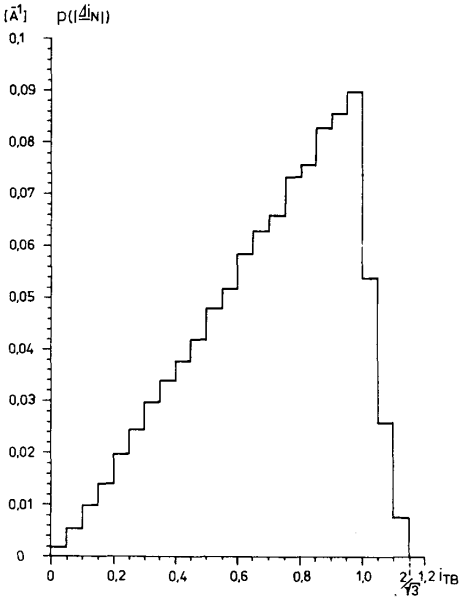

Fig. 10. Predictive controller: Distribution density of $|\Delta\underline{i}_N|$; (f_N = 50 Hz, $U_{N,eff}$ = 220 V, $|\underline{i}_N^*|$ = 25 A, U_Z = 620 V, L = 6.2 mH, i_{TB} = 2 A). $2i_{TB}/\sqrt{3}$ is radius of the "outer circle" of tolerance area. Because tolerance area is not left (due to constraint of optimization) $p(|\Delta\underline{i}_N|) = 0$ is valid for $|\Delta\underline{i}_N| > 2i_{TB}/\sqrt{3}$.

For the dependencies of the characteristic quantities on the system parameters (Figs. 10, 15 or [3], respectively) essentially the same is valid as is given for the hysteresis controller. The characteristic of the switching frequency as a function of the mains voltage amplitude can be explained as follows: for small ac voltages the freewheeling state is taken on due to the optimization in a preferred manner (Fig. 15); this is opposed to the hysteresis controller. The system remains in the freewheeling state for a longer period of time due to the small $[d(\Delta\underline{i}_N)/dt]_{0,7}$; this results in a low switching frequency. If $|\underline{u}_N|$ lies close to $|\underline{u}_U|$ there again switching states occur (close to the mains voltage vector) showing a low $d(\Delta\underline{i}_N)/dt$; this results in a decrease of the switching frequency f_s for higher ac voltages. For $|\underline{u}_U| \approx 2\,|\underline{u}_N|$ "resonant cycles" similar as in the case of the hysteresis controller can be observed, despite the optimization performed. These cycles result in an increased f_s, which can be explained by the then given high degree of symmetry of the $[d(\Delta\underline{i}_N/dt)]k_l$. The switching frequency trend therefore can only be described as approximately smooth.

V. Off-Line Optimized Predictive Controller—Control Table

As mentioned in Section IV, the predictive controller requires knowledge about the instantaneous system state k to select the optimal new switching state k_l. In the stationary case considered here the system state is characterized by $\underline{u}_N$, $\underline{i}_N^*$, $\Delta\underline{i}_N$ and the switching state k existing until now. According to (3) $\underline{i}_N^*$ exerts only very small influence on the $[d(\Delta\underline{i}_N)/dt]k_l$ (and consequently on f_s, Fig. 11) for small values of L (as mostly given in real systems), because then $|\underline{u}_N| \gg \omega_N L|\underline{i}_N^*|$. The inductive voltage drop essentially causes only a rotation of $\underline{u}_N$ by an angle of a few degrees. This is of little significance because $\underline{u}_U$ can assume only six different directions with an angle of 60° between them. Therefore, the switching decision of the predictive controller is almost independent of the magnitude I_N of $\underline{i}_N$ and primarily determined by $\underline{u}_N$, $\Delta\underline{i}_N$ and k.

For a given value of the mains voltage therefore the optimal k_l can be given by eight tables for the different values of k if a sufficiently fine discretization of $\phi\underline{u}_N$ and $\phi\underline{i}_N$ (arguments of $\underline{u}_N$ and $\Delta\underline{i}_N$) is made (6° in Fig. 12). For a given output state k only such new states (k_l) are listed for which the trajectory corresponding to k would cross the tolerance region boundary (hexagon) from the inside. Only those values are needed if $\Delta\underline{i}_N$ is controlled within the hexagon (which is guaranteed by the working principle of the predictive controller). The other locations in the table (indicated by "8" in Fig. 12) could be filled, e.g., by $k_l = k$ because k there leads (already) back into the hexagon without making switching necessary.

As shown in Fig. 12, different k_l appear (with good approximation) only in 30°-segments of the table. This can be explained basically by the 30° symmetry of the tolerance region in connection with the 60° discrete directions of $\underline{u}_U$. The expectation being obvious therefore, namely that the predictive controller can be described by switching tables of relatively less extent (Fig. 13), is proven by simulation. The high effort connected with the ON-line optimizing predictive controller [2] can be avoided by an OFF-line optimization stored in tables (for different k) with relatively small storage requirements.

The problem of making one (medium) switching decision for a whole 30° × 30° segment is, besides the then

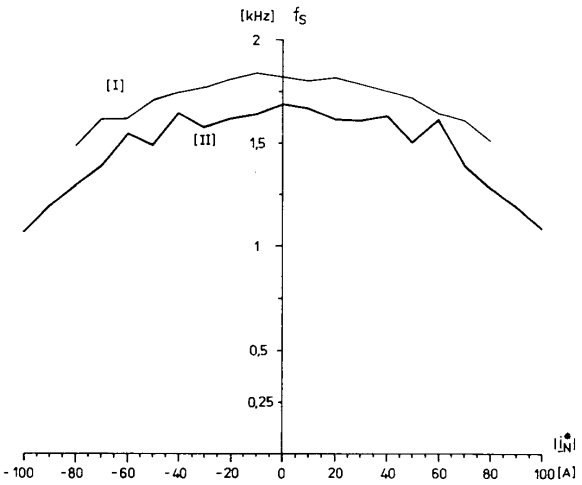

Fig. 11. Switching frequency as function of current reference value $|\underline{i}_N^*|$; (f_N = 50 Hz, U_{Neff} = 220 V, U_Z = 620 V, i_{TB} = 2 A, L = 6.2mH). $|\underline{i}_N^*| < 0$ stands for $\psi = 180°$ (power conversion from the dc to the ac side). I. Predictive controller; II. Hysteresis controller. ("Measuring points": every multiple of 10 A, linear interpolation); f_s decreases with increasing $|\underline{i}_N^*|$; this can be explained by then higher counter voltage $\underline{u}_{U,i}$ (increased voltage across L).

not always given optimality, that the chosen k_I does not guide $\Delta\underline{i}_N$ back into the hexagon in each case. The second control concept which has to be superimposed on the predictive controller to handle transient conditions (see Section IV) then also has to interact occasionally for stationary working conditions in order to correct the control error. An exact definition of the maximum control error therefore is not possible. As an analysis of the distribution density of $|\Delta\underline{i}_N|$ shows (Fig. 14), the deviation from the behavior of the on-line optimizing predictive controller is relatively small. This is because the maximum value of $\Delta\underline{i}_N$ exceeds i_{TB} only by a small amount and this also occurs very seldom. An essential influence on the rms value of $\Delta\underline{i}_N$ thereby is not given.

With a predictive controller a significant reduction of the switching frequency (compared to the hysteresis controller) is possible especially for low frequencies of the ac side (assumption: $|\underline{u}_N|/\omega_N$ = constant resulting in an approximately constant flux of an ac machine). As described before this is achieved due to the then very small $d(\Delta\underline{i}_N)/dt$ of the freewheeling states. As the investigations show, a controller with a 30° discrete switching table (established, e.g., for f_N = 5 Hz, Fig. 13) may lower the switching frequency even beneath that of the ON-line predictive controller (Fig. 15). This phenomenon can be explained by the fact that the optimization is performed only according to the "local" switching frequency; furthermore, the "resonant cycles" of the ON-line predictive controller (described in Section IV) cause an increase of the switching frequency as compared to its (global) minimum possible value. Moreover, due to these cycles the free-wheeling trajectory will be situated in a preferred manner close to the tolerance area boundaries which would increase the rms value of $\Delta\underline{i}_N$. The "disturbed" optimization given by the not exact (not "sufficiently" fine) switching table avoids such resonant cycles for the table-based controller. The investigations performed show that the table proves to be extremely robust and leads (for a wide ac voltage region) to switching frequencies being smaller than those of the ON-line predictive controller with an approximately equal rms value of $\Delta\underline{i}_N$ (Figs. 15 and 16). In the vicinity of $|\underline{u}_U| \approx 2|\underline{u}_N|$ the switching table has only limited validity (because it is based, as mentioned before, on f_N = 5 Hz). The superimposed control system (in the present case a hysteresis controller) has to interact more and more to correct the control error. The switching frequency lies, as that of the on-line predictive controller, of the hysteresis controller. Basically then the effect of an optimization is not noticeable because the magnitudes of the $[d(\Delta\underline{i}_N)/dt]k_I$ are not very different. Moreover, the (locally effective) optimization criterion cannot eliminate "resonant cycles" appearing due to symmetries [3].

In practical applications a substitution of the ON-line predictive controller (avoiding the high effort connected with it) by a table based controller is possible. Then for lower ac voltages the switching decisions of this controller are taken from an OFF-line optimized switching table; at higher ac voltages the system is switched over to the superimposed hysteresis controller. This transition therefore can be performed quasi continuously because the switching decisions for the hysteresis controller can also be put into tables easily; the "switching over" only means an exchange of the switching table. "Switching over" takes place in the case of operation based on the optimized control table also, in the case that the optimized switching decision does not lead back the $\Delta\underline{i}_N$ into the tolerance area.

The complex plane is divided into 19 segments (sectors) by the six thresholds (Fig. 17) which are defined by corresponding $\Delta i_{N,R}$, $\Delta i_{N,S}$, $\Delta i_{N,T}$. With an additional evaluation of $\Delta i_{N,R} - \Delta i_{N,S}$, $\Delta i_{N,S} - \Delta i_{N,T}$ and $\Delta i_{N,T} - \Delta i_{N,R}$ a 30° sector for $\Delta\underline{i}_N$ (necessary for the table based controller) can be determined by a simple comparator circuit. The evaluation of the $\underline{u}_N$ is also performed via the phase quantities $u_{N,R}$, $u_{N,S}$, $u_{N,T}$.

As mentioned before, the table based operation is switched over to a pure hysteresis controller operating at higher ac voltages. This requires establishing of $|\underline{u}_N|$ by (1) in Fig. 18 (e.g., a simple rectifier followed by a comparator). If the table-based controller is part of a drive control system the ac voltage ("mains") is realized by the counter emf of the motor; this voltage therefore is not accessible directly but often calculated anyhow to control the flux of the motor. If this is done by digital control (1) and (2) of Fig. 18 can be omitted.

The table based controller shown in Fig. 18 basically represents a synchronous state sequencer. This requires a clock-synchronous transfer of the input variables. To detect the crossed threshold the sector number s_i (supplied by $\Delta\underline{i}_N$-comparators I and II) is compared with $s_i - 1$ (the

X-AXIS: $\varphi_{\Delta i_N}$
Y-AXIS: $\varphi_{\underline{u}_N}$

	0	30	60	90	120	150	180	210	240	270	300	330
336	88888	88888	88888	88888	88888	88888	88888	88888	88888	88888	88888	88888
342	88888	88888	88888	88888	88888	88888	88888	88888	88888	88888	88888	88888
348	88888	88888	88888	88888	88888	88888	88888	88888	88888	88888	88888	88888
354	88888	88888	88888	88888	88888	88888	88888	88888	88888	88888	88888	88888
0	88888	88888	88888	88888	88888	88888	88888	88888	88888	88888	88888	88888
6	88888	88888	88888	88888	88888	88888	88888	88888	88888	88888	88888	88888
12	88888	88888	88888	88888	88888	88888	88888	88888	88888	88888	88888	88888
18	88888	88888	88888	88888	88888	88888	88888	88888	88888	88888	88888	88888
24	88888	88888	88888	88888	88888	88888	88888	88888	88888	88888	88888	88888
30	30000	00000	00000	00000	03333	33333	33333	33333	33333	33333	33333	33333
36	30000	00000	00000	00000	00000	00003	33333	33333	33333	33333	33333	33333
42	30000	00000	00000	00000	00000	00000	03333	33333	33333	33333	33333	33333
48	30000	00000	00000	00000	00000	00000	03333	33333	33333	33333	33333	33333
54	30000	00000	00000	00000	00000	00000	03333	33333	33333	33111	11111	11133
60	10000	00000	00000	00000	00000	00000	03333	33311	11111	11111	11111	11111
66	10000	00000	00000	00000	00000	00000	01111	11111	11111	11111	11111	11111
72	10000	00000	00000	00000	00000	00000	01111	11111	11111	11111	11111	11111
78	10000	00000	00000	00000	00000	00000	01111	11111	11111	11111	11111	11111
84	10000	00000	00000	00000	00000	00000	01111	11111	11111	11111	11111	11111
90	11111	11111	10000	00000	00000	00000	01111	11111	11111	11111	11111	11111
96	11111	11111	10000	00000	00000	00000	00000	00000	01111	11111	11111	11111
102	55555	55511	10000	00000	00000	00000	00000	00000	01111	11111	11111	15555
108	55555	55555	50000	00000	00000	00000	00000	00000	01111	11115	55555	55555
114	55555	55555	50000	00000	00000	00000	00000	00000	01555	55555	55555	55555
120	55555	55555	50000	00000	00000	00000	00000	00000	05555	55555	55555	55555
126	55555	55555	40000	00000	00000	00000	00000	00000	05555	55555	55555	55555
132	55544	44444	40000	00000	00000	00000	00000	00000	05555	55555	55555	55555
138	44444	44444	40000	00000	00000	00000	00000	00000	04445	55555	55555	44444
144	44444	44444	40000	00000	00000	00000	00000	00000	04444	44444	44444	44444
150	44444	44444	44444	44444	40000	00000	00000	00000	04444	44444	44444	44444
156	44444	44444	44444	44444	40000	00000	00000	00000	00000	00000	04444	44444
162	44444	44444	44444	44444	40000	00000	00000	00000	00000	00000	04444	44444
168	44444	44444	44444	44444	40000	00000	00000	00000	00000	00000	04444	44444
174	44444	44444	44444	44444	40000	00000	00000	00000	00000	00000	04444	44444
180	44444	44444	44446	66666	60000	00000	00000	00000	00000	00000	04444	44444
186	44444	66666	66666	66666	60000	00000	00000	00000	00000	00000	06664	44444
192	66666	66666	66666	66666	60000	00000	00000	00000	00000	00000	06666	66666
198	66666	66666	66666	66666	60000	00000	00000	00000	00000	00000	06666	66666
204	66666	66666	66666	66666	66600	00000	00000	00000	00000	00000	06666	66666
210	66666	66666	66666	66666	66666	66666	60000	00000	00000	00000	06666	66666
216	88888	88888	88888	88888	88888	88888	88888	88888	88888	88888	88888	88888
222	88888	88888	88888	88888	88888	88888	88888	88888	88888	88888	88888	88888
228	88888	88888	88888	88888	88888	88888	88888	88888	88888	88888	88888	88888
234	88888	88888	88888	88888	88888	88888	88888	88888	88888	88888	88888	88888
240	88888	88888	88888	88888	88888	88888	88888	88888	88888	88888	88888	88888
246	88888	88888	88888	88888	88888	88888	88888	88888	88888	88888	88888	88888
252	88888	88888	88888	88888	88888	88888	88888	88888	88888	88888	88888	88888
258	88888	88888	88888	88888	88888	88888	88888	88888	88888	88888	88888	88888
264	88888	88888	88888	88888	88888	88888	88888	88888	88888	88888	88888	88888
270	88888	88888	88888	88888	88888	88888	88888	88888	88888	88888	88888	88888
276	88888	88888	88888	88888	88888	88888	88888	88888	88888	88888	88888	88888
282	88888	88888	88888	88888	88888	88888	88888	88888	88888	88888	88888	88888
288	88888	88888	88888	88888	88888	88888	88888	88888	88888	88888	88888	88888
294	88888	88888	88888	88888	88888	88888	88888	88888	88888	88888	88888	88888
300	88888	88888	88888	88888	88888	88888	88888	88888	88888	88888	88888	88888
306	88888	88888	88888	88888	88888	88888	88888	88888	88888	88888	88888	88888
312	88888	88888	88888	88888	88888	88888	88888	88888	88888	88888	88888	88888
318	88888	88888	88888	88888	88888	88888	88888	88888	88888	88888	88888	88888
324	88888	88888	88888	88888	88888	88888	88888	88888	88888	88888	88888	88888
330	88888	88888	88888	88888	88888	88888	88888	88888	88888	88888	88888	88888

Fig. 12. Switching table of predictive controller; horizontal: $\phi\Delta i_N$, vertical: ϕu_N (both given in steps of 6°). (f_N = 5 Hz, $U_{N,\text{eff}}$ = 22 V, $|\underline{i}_N^*|$ = 25 A, U_Z = 620 V, i_{TB} = 2 A, L = 6.2 mH, instantaneous switching state k = 2). Table provides optimal new switching state k_l.

$\varphi_{\underline{u}_N}$ \ $\varphi_{\Delta \underline{i}_N}$											
	2	2	2	2	2	2	2	2	2	2	2
	2	2	2	2	2	2	2	2	2	2	2
	0	0	0	0	0	0	3	3	3	3	3
	0	0	0	0	0	0	1	1	1	1	1
	5	5	0	0	0	0	0	0	1	1	5
	4	4	0	0	0	0	0	0	4	5	5
	4	4	4	4	0	0	0	0	0	0	4
	6	6	6	6	0	0	0	0	0	0	6
	2	2	2	2	2	2	2	2	2	2	2
	2	2	2	2	2	2	2	2	2	2	2
	2	2	2	2	2	2	2	2	2	2	2
	2	2	2	2	2	2	2	2	2	2	2

Fig. 13. Simplified switching table derived from Fig. 12; resolution of 30° for $\phi\Delta\underline{i}_N$ (horizontal) and $\phi\underline{u}_N$ (vertical).

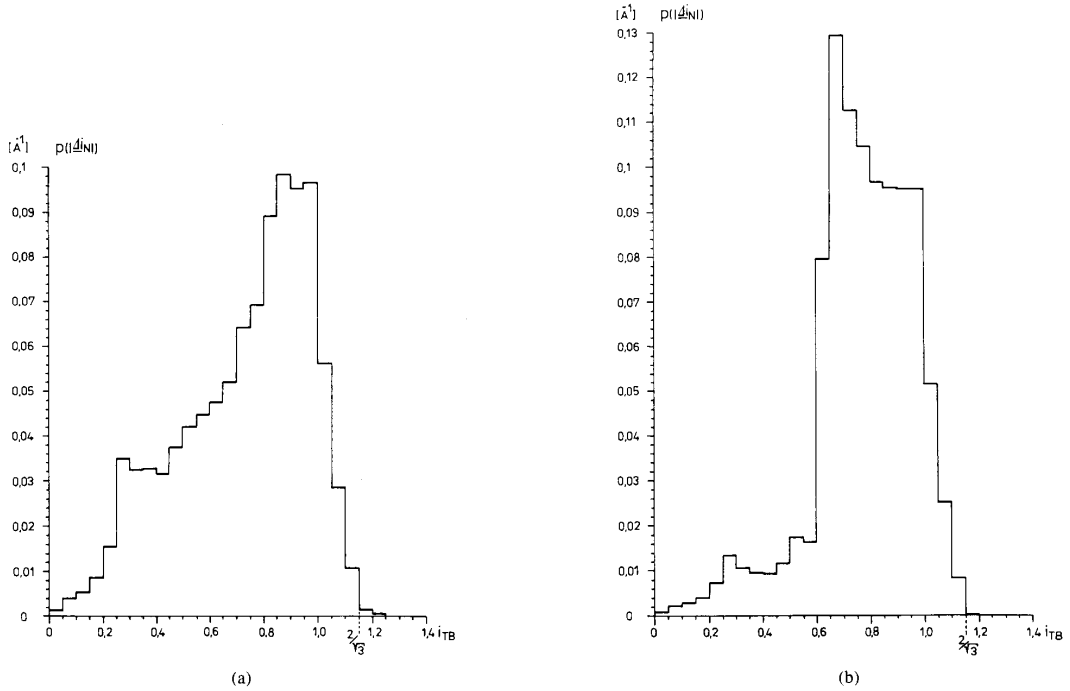

Fig. 14. Distribution density of $|\Delta\underline{i}_N|$: (f_N = 5 Hz, $U_{N,\text{eff}}$ = 22 V, $|\underline{i}_N^*|$ = 25 A, U_Z = 620 V, i_{TB} = 2 A, L = 6.2 mH, instantaneous switching state k = 2); (a) (left) : off-line optimized control table; (b) (right): predictive controller. Smaller $\Delta i_{N,\text{eff}}$ of (a) compared to (b) (see Fig. 15, f_N = 5 Hz) is due to "disturbed" optimization of table based controller (avoidance of "resonant" switching cycles).

sector number delayed by one clock cycle) by the $\Delta\underline{i}_N$-encoder (8). It is assumed that the clock frequency is sufficiently high that within one clock cycle only transfers between directly neighboring sectors are possible. Then this information can be expressed as a 6-bit data word if the information for the predictive controller is included. The $\Delta\underline{i}_N$-comparator I (4) forms a tolerance region which is tilted by 30° compared to that region determined by (3) (Fig. 19). (From this there follows the possibility to evaluate $\phi\Delta\underline{i}_N$ in 30° segments.) The $\Delta\underline{i}_N$-encoder II (realized as 32k-bit EPROM such as encoder I) transfers the information concerning $\Delta\underline{i}_N$ to the control table if the system trajectory moves from the hexagon into a neighboring sector (this means that a "predictive controller decision" has to be made). If the control error cannot be turned back by that, boundaries of outer sectors will be crossed. The

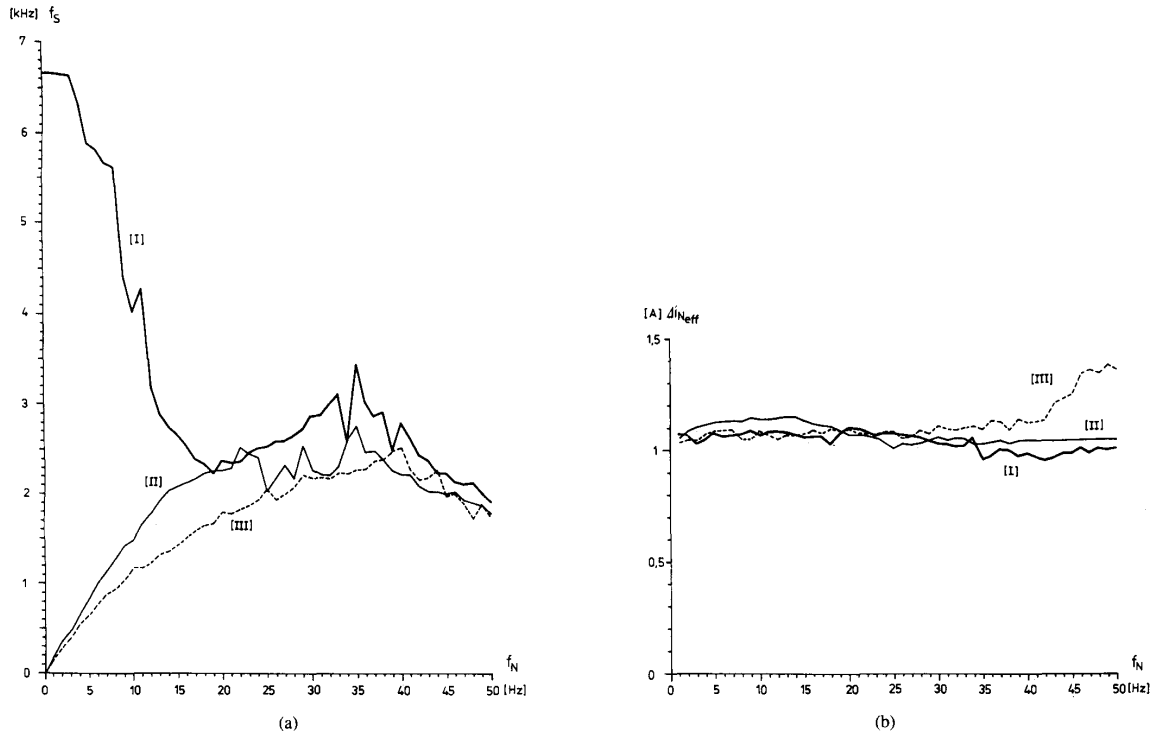

Fig. 15. Comparison of switching frequencies and rms values of Δi_N for control concepts treated: I. Hysteresis controller (i_{TB} = 1.67 A) II. Predictive controller (i_{TB} = 2 A) III. Optimized control table (i_{TB} = 2 A), optimized for f_N = 5 Hz, $U_{N,\text{eff}}$ = 22 V. An approximately equal rms value of $\Delta i_{N,\text{eff}}$ is achieved with mentioned i_{TB} values. If i_{TB} is adapted to keep $\Delta i_{N,\text{eff}}$ constant exactly, $f_s = f_s(f_N)$ would be smoother than shown. ($|\underline{i}_N^*|$ = 25 A, U_Z = 620 V, L = 6.2 mH, $U_{N,\text{eff}}/f_N$ = constant = 220 V/50 Hz).

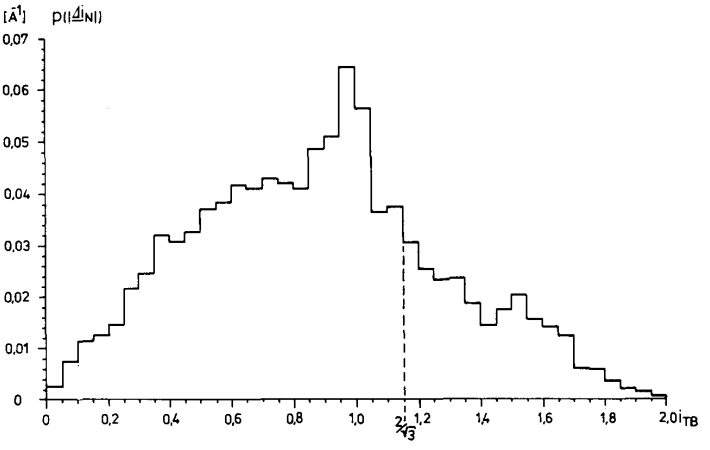

Fig. 16. Table-based controller (optimization for f_N = 5 Hz, $U_{N,\text{eff}}$ = 22 V): Distribution density of $|\Delta \underline{i}_N|$; (f_N = 50 Hz!, $U_{N,\text{eff}}$ = 220 V, $|\underline{i}_N^*|$ = 25 A, U_Z = 620 V, i_{TB} = 2A, L = 6.2 mH).

information that hysteresis controller operation has to be selected in this case is also contained in the encoder II (9) output (6-bit). The pure hysteresis controller operation for higher ac voltages is selected by (1).

The output of a new switching state is delayed by one clock cycle such that the previous switching state (required for predictive controller decisions) is available to the control table. Due to the realization as a synchronous

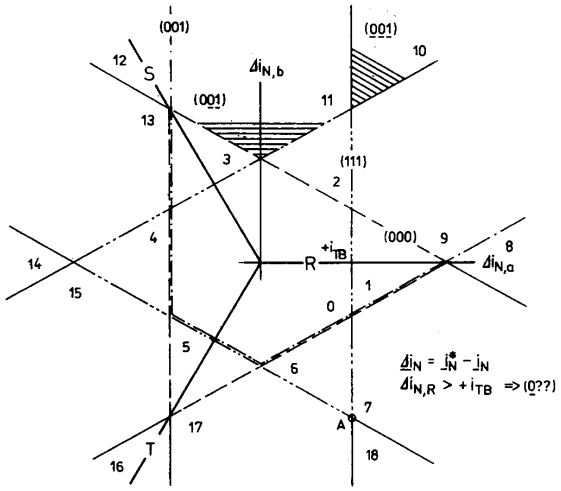

Fig. 17. Tolerance area for space vector representation of Δi_N.

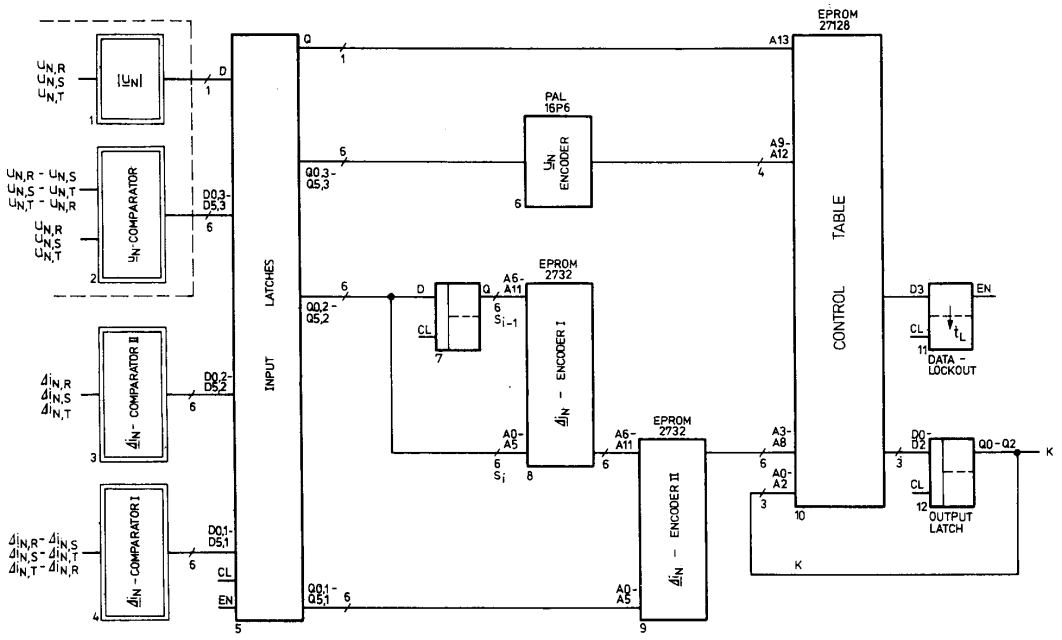

Fig. 18. Realization of off-line optimized (table-based) predictive controller as synchronous state sequencer.

state sequencer a change of the system variables is recognized within one clock cycle. It leads to the output of a new switching state and activates the data-lockout circuit (11). The data-lockout (realized as a clock-synchronous monostable multivibrator) temporarily inhibits the update of the system state variables (5). This is required because the controlled system responds to the new switching state (output by the controller) only after the converter delay time. A change of the control output during this time is not meaningful. The converter delay time therefore is the minimum value for the data-lockout.

VI. Conclusion

The basic idea of the predictive controller represents an attractive method for minimization of the switching frequency in ON-OFF controlled systems. As shown in this paper, the problem lies in selecting the proper optimization criterion together with practicable constraints. Under consideration of an economical realization only a local optimization (according to a steepest descent method) is possible due to the simplicity of the mathematical conditions given in that case. This leads to a substantial im-

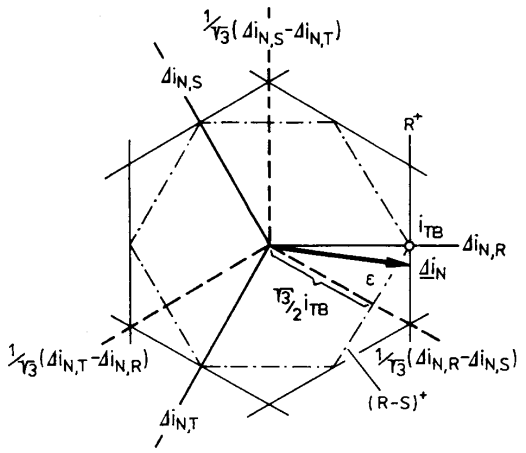

Fig. 19. Superposition of two tolerance areas (I and II) tilted 30° with respect to each other for receiving a 30° resolution for ϕi_N; for case shown here position of Δi_N can be clearly related to corresponding 30° sector given by $R+$ and $(R-S)+=1$.

provement as compared to the simple hysteresis controller in such parameter regions where switching states can be assumed which have great influence on the variable to be optimized. (This means that the basic condition for good optimizability is given.) However, it is shown that in the case considered here the predictive controller does not justify the high effort of an ON-line realization.

With a system being of much simpler structure, consisting basically of a switching table gained from OFF-line optimization, the selection of the "optimal" switching decision (according to the points of view mentioned) cannot be guaranteed in any case. However, this seeming disadvantage altogether leads to a system behavior that—for a wide range of the parameters—lies closer to the global optimum than for the predictive controller. This is based on the fact that the predictive controller optimizes the system behavior only within a very limited time interval. Therefore, the optimum evaluated by the predictive controller is not the global optimum. It is shown that the proposed OFF-line optimized table based controller comes closer to the global optimum.

REFERENCES

[1] H. Ertl, J. W. Kolar, and F. Zach, "Analysis of different current control concepts for forced commutated rectifier (FCR)," in *Proc. 11th PCI Conf.*, Munich, Germany, June 17-19, 1986, pp. 195-217.

[2] Holtz, J., and S. Stadfeld, "A PWM inverter drive system with on-line optimized pulse patterns," in *Proceedings First European Conf. on Power Electronics and Applications*, Brussels, Belgium, Oct. 16-18, 1985, vol. 2, pp. 3.21-3.25.

[3] H. Ertl, J. W. Kolar, and F. C. Zach, "Comparison of simple and optimized on-off current controllers for three-phase systems," in *Proceedings 13th PCI Conf.*, Munich, May 11-13, 1987, pp. 66-83.

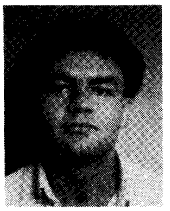

Johann W. Kolar (M'89) was born in Upper Austria on July 15, 1959. He is with the Power Electronics Section of the Technical University Vienna. He is currently working on the Ph.D. degree in the area of control optimization of single-phase and three-phase PWM rectifier systems.

He also does research in the areas of inverter and converter development and the theoretical analysis of power electronic systems and is the author of numerous scientific papers and patents.

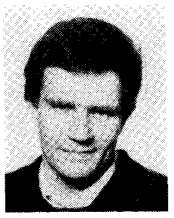

Hans Ertl was born in Upper Austria on May 28, 1957. He received the Dipl.Ing. (M.Sc.) degree from the Technical University Vienna, Austria, in 1984. As a Scientific Assistant of the Power Electronics Section, he presently is finishing his Ph.D. thesis in the area of three-phase PWM converter systems.

He also does research concerning the analysis and design of switched mode power supplies and is the author of various scientific papers and patents.

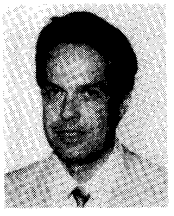

Franz C. Zach (M'83) was born in Vienna, Austria, on December 5, 1942. He received the Dipl.Ing. (M.Sc.) and Ph.D. degrees (cum laude) from the University of Technology, Vienna, Austria, in 1965 and 1968, respectively.

From 1965 to 1969 he was a Scientific Assistant in Vienna, and from 1969 to 1972 he was with the NASA Goddard Space Flight Center in Greenbelt, MD (Washington, DC). In 1972 he returned to Austria to become Associate Professor for Power Electronics at the Vienna University of Technology. There he has been heading the Power Electronics Group since 1974. He is the author of numerous technical/scientific papers and of two books on automatic control and on power electronics. His current activities lie in power electronics and associated controls, especially as used for variable-speed ac and dc motor drives and for power supplies. He is also involved in extensive industrial work in these areas.